Development 123, 217-227
Printed in Great Britain © The Company of Biologists Limited 1996
DEV3336

Mutations affecting neural survival in the zebrafish *Danio rerio*

Salim Abdelilah, Eliza Mountcastle-Shah, Michele Harvey, Lilianna Solnica-Krezel, Alexander F. Schier, Derek L. Stemple, Jarema Malicki, Stephan C. F. Neuhauss, Fried Zwartkruis*, Didier Y. R. Stainier†, Zehava Rangini‡ and Wolfgang Driever§

Massachusetts General Hospital and Harvard Medical School, Building 149, 13th Street, Charlestown, MA 02129, USA

*Present address: Laboratory for Physiological Chemistry, Utrecht University, Universiteitsweg 100, 3584 CG Utrecht, The Netherlands
†Present address: Department of Biophysics and Biochemistry, University of California San Francisco, CA 94143, USA
‡Present address: Department of Oncology, Sharett Institute, Hadassah Hospital, Jerusalem 91120, Israel
§Author for correspondence (e-mail: driever@helix.mgh.harvard.edu)

SUMMARY

Programmed cell death is a prominent feature of normal animal development. During neurogenesis, naturally occurring cell death is a mechanism to eliminate neurons that fail to make appropriate connections. To prevent accidental cell death, mechanisms that trigger programmed cell death, as well as the genetic components of the cell death program, are tightly controlled.

In a large-scale mutagenesis screen for embryonic lethal mutations in zebrafish *Danio rerio* we have found 481 mutations with a neural degeneration phenotype. Here, we present 50 mutations that fall into two classes (termed spacehead and fala-like) that are characterized by two main features: first, they appear to affect cell survival primarily within the neuroectodermal lineages during somitogenesis, and second, they show an altered brain morphology at or before 28 hours of development. Evidence for the specificity of cell death within the central nervous system comes from visual inspection of dying cells and analysis of DNA fragmentation, a process associated with apoptotic cell death. In mutants, the level of dying cells is significantly increased in brain and spinal cord. Furthermore, at the end of somitogenesis, the cell count of radial glia and trigeminal neurons is reduced in some mutants of the spacehead class.

A variety of neurodegenerative disorders in mouse and humans have been associated with abnormal levels of programmed cell death within the central nervous system. The mutations presented here might provide a genetic framework to aid in the understanding of the etiology of degenerative and physiological disorders within the CNS and the activation of inappropriate programmed cell death.

Key words: zebrafish, development, CNS, programmed cell death, degeneration

INTRODUCTION

In the vertebrate nervous system, an excess number of neurons arises during neurogenesis. Only about half of these neurons will survive past early development (Hamburger and Levi-Montalcini, 1949). This surplus of neurons is thought in part to ensure the formation of correct synaptic connections between neurons and their targets. The survival of neurons appears to depend on the availability of specific neurotrophic factors provided by their target cells (Cohen et al., 1954; Levi-Montalcini, 1987; Barde, 1989; Oppenheim, 1991; Thoenen, 1991; Hamburger, 1992; Raff et al., 1993). The hypothesis of a neurotrophic strategy of neuronal survival has been tested by the analysis of mouse strains with targeted deletions of genes for a variety of neurotrophic factors and their receptors, such as NGF, BDNF, *trk*A, *trk*B, *trk*C, and p75 (Lee et al., 1992; Klein et al., 1993; Crowley et al., 1994; Ernfors et al., 1994; Jones et al., 1994; Klein et al., 1994; Smeyne et al., 1994; for review see Klein, 1994). These targeted mutations have demonstrated that the survival of specific neuronal cell types, predominantly within the peripheral nervous system, depends on the presence of the neurotrophin family signaling pathways.

Neuronal loss during development has been referred to as naturally occurring neuronal death (for review see Jessell, 1991). Moreover, it has been found that this form of cell death is executed by an active developmental program (Saunders, 1966; Truman, 1984; Raff, 1992; Raff et al., 1993). In particular, apoptosis, a morphologically distinct form of programmed cell death, has been proposed as an essential mechanism of cellular suicide during development (Kerr et al., 1972; Wyllie et al., 1980; Ellis et al., 1991; Raff, 1992; Schwartz and Osborne, 1994). Cells dying by an apoptotic mechanism are characterized by a condensation of both nucleus and cytoplasm, often followed by fragmentation of the entire cell (Robertson and Thomson, 1982). An additional feature of apoptosis is the activation of nucleases which results in the degradation of chromosomal DNA into smaller fragments (Wyllie et al., 1980). Genetic analysis of cell death in *C. elegans* has identified a number of genes, such as *ced-3*, *ced-4*, and *ced-9*, involved in the control and execution of apoptosis (Ellis and Horvitz, 1986). The iden-

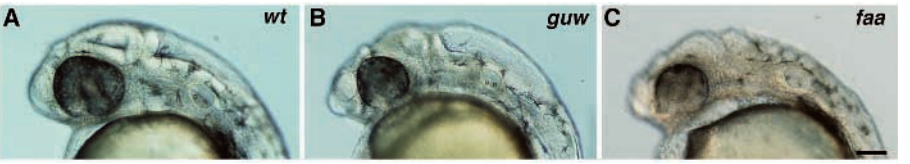

Fig. 1. Head phenotypes of mutants of the spacehead and fala-like classes at 30 hpf. (A) Wild-type. (B) *gumowy*^{m585}. (C) *fala*^{m249} Lateral view of live embryos. Transmitted light, anterior to the left. Scale bar, 100 μm.

tification of vertebrate homologues of *ced-3* and *ced-9* indicates that the genetic pathway of apoptotic cell death is conserved among metazoans (Yuan et al., 1993; Hengartner and Horvitz, 1994; for review see Vaux et al., 1994; Steller, 1995; Wyllie, 1995).

Recently, attention has been focused on the mechanisms that activate apoptotic cell death. In mice, a number of mutations affecting neural survival have been identified, some of which are clearly linked to increased apoptotic levels (Chang et al., 1993; Norman et al., 1995). Since there is no evidence for defective neurotrophic signaling in these mutations, a number of possibly different genetic defects appear to cause the abnormal activation of apoptotic cell death within the neural lineages. Furthermore, abnormal levels of apoptotic cell death have been implicated in human neurodegenerative disorders such as Alzheimer's disease, Parkinson's disease, amyotrophic lateral sclerosis (ALS), spinal muscular atrophy, and cerebellar degeneration (for review see Thompson, 1995). A variety of cell-autonomous and cell-nonautonomous factors might be involved in the etiology of these diseases (Choi, 1992). The analysis of a range of different genetic defects which can result in apoptotic cell death within the central nervous system (CNS) might further our understanding of the development of neurodegenerative diseases.

The zebrafish *Danio rerio* is exceptionally well suited for developmental neurobiological studies as well as genetic analysis (Streisinger et al., 1981; Kimmel and Westerfield, 1990; Mullins et al., 1994; Solnica-Krezel et al., 1994; Kimmel et al., 1995). To date, only one mutation affecting the survival within the neuroectodermal lineages has been described (Grunwald et al., 1988). It has been suggested that the *ned1*^{b39} mutation predominantly affects neurons arising after the first wave of primary neurons.

We have performed a large-scale mutagenesis screen for embryonic and early larval lethal mutations in zebrafish *Danio rerio* (Driever et al., 1996). Among the 2383 mutations isolated, we have identified 481 zygotic recessive mutations that lead to increased levels of cell death within the CNS at various stages of early development. All of these mutations were characterized as belonging to one of three categories, the largest of which, with 398 mutations, results in widespread cell death within the CNS, and is detectable by visual inspection only after the end of somitogenesis, without expressing early morphological abnormalities. A second category comprises 33 mutations that result in locally restricted or transiently occurring cell death within the CNS and do not lead to early morphological abnormalities either. In this paper we present 50 mutations of a third category, which are defined by the early onset, during somitogenesis, of significantly increased cell death, and by distinct sets of morphological abnormalities. Analysis of DNA fragmentation (Gavrieli et al., 1992; Zakeri et al., 1993), indicates similarities among two classes of mutations with increased region-specific cell death in the brain and spinal cord. In order to illustrate that CNS-restricted increased cell death is only one of several different patterns of cell death possible in zebrafish, we describe a third class of miscellaneous early degenerative mutations that lead to a variety of different patterns of cell death and developmental retardations.

MATERIAL AND METHODS

Fish strains

Mutations were induced and isolated as described by Solnica-Krezel et al. (1994); Driever et al. (1996). For outcrosses of mutations, either AB strains that were obtained from the University of Oregon in Eugene, and bred in our facility for several generations, or TüAB hybrid strains that were obtained from the Max-Planck Institute for Developmental Biology in Tübingen/Germany, were used.

Identification of mutations and complementation analysis

Mutations were identified at the end of somitogenesis at 24-28 hours postfertilization (hpf) at 28°C by visual inspection under a dissecting microscope. Complementation analysis was performed by screening a minimal number of 30 embryos per complementation cross at 28 hpf. Within the spacehead class, out of a total of 903 necessary complementation crosses, 78 were not completed. On average, one non-complementing cross was found every 46 crosses. Therefore, only one or two additional non-complementing crosses would be expected

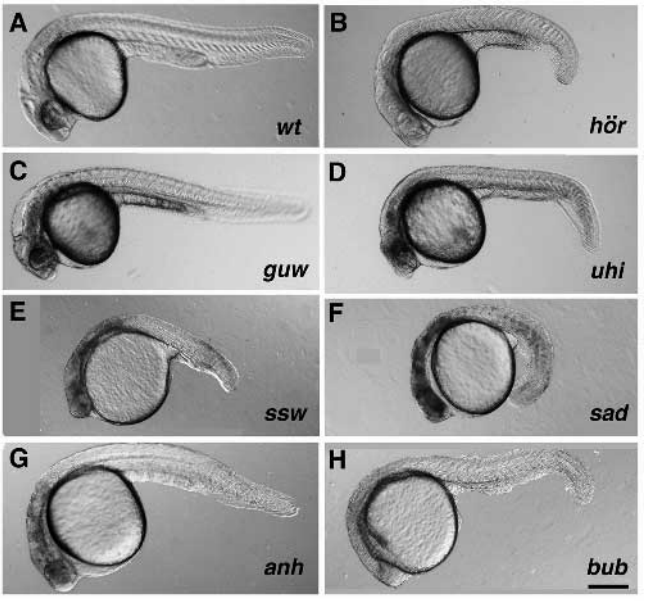

Fig. 2. Mutants of the spacehead and miscellaneous early degeneration classes at 28 hpf. (A) Wild-type. (B) *hörnle*^{m274}. (C) *gumowy*^{m585}. (D) *uchu hikoushi*^{m172}. (E) *sideswipe*^{m762}. (F) *stop and drop*^{m367}. (G) *anhalter*^{m767}. (H) *bubbles*^{m450}. Lateral view of live embryos. Transmitted light, anterior to the left. Scale bar, 250 μm.

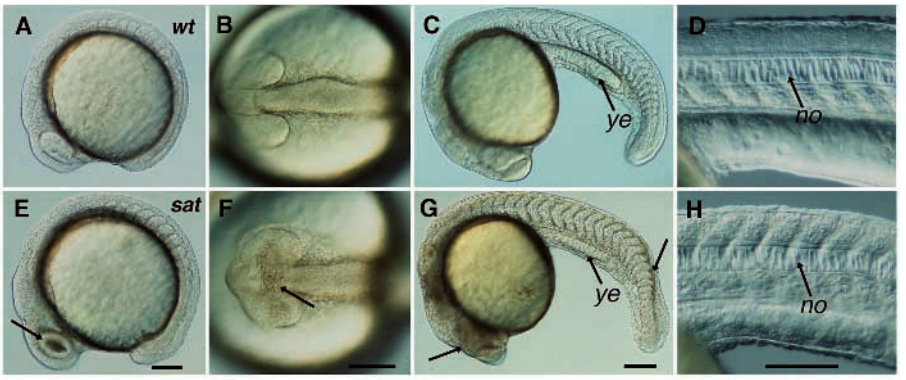

Fig. 3. Early development of spacehead mutant *saturn*^{m465}. (A-D) Wild-type. (E-H) *saturn*^{m465}. (A,B,E,F) 12-somite stage. (C,D,G,H) 23/24-somite stage. (A,C,D,E,G,H) Lateral view of live embryo. (B,F) Dorsal view onto brain. (E,F,G) Arrows indicate regions of visible degeneration. Transmitted light, anterior to the left. no, notochord; ye, yolk extension. Scale bars, 100 μm.

among the following crosses that have not been performed (crosses are listed in numerical order with the smallest mutation number first): *m172×488; m172×613; m250×488; m250×513; m250×613; m331×488; m331×513; m331×613; m332×488; m332×613; m383×488; m383×513; m383×514; m383×613; m404×488; m404×513; m404×613; m409×488; m409×613; m461×513; m461×613; m481×488; m481×513; m481×613; m488×492 m488×506; m488×513; m488×514; m488×584; m488×613; m488×728; m488×766; m492×513; m492×613; m506×513; m506×613; m513×514; m513×613; m513×766; m514×613; m584×613; m613×728; m613×766*.

Mutations m590 and m685 were only tested for complementation in the following crosses: *m332×590; m445×590, m465×590; m479×590; m481×590; m584×590; m590×691; m590×727; m590×728; m590×733; m97×685; m221×685; m332×685; m333×685; m445×685; m465×685; m479×685; m492×685; m591×685; m685×691; m685×727; m685×728*.

In the fala-like class, mutation *m569* was only tested for complementation in the following crosses: *m83×569; m175×569.*

Immunohistochemistry and whole-mount in situ hybridization

Embryos were staged according to Kimmel et al. (1995). After fixation overnight in 4% paraformaldehyde in PBS, embryos were transferred and stored in methanol at –20°C. Whole-mount in situ hybridizations were performed as previously described (Oxtoby and Jowett, 1993). Dioxigenin-labelled RNA was transcribed according to the manufacturer's instructions (Dig RNA Labeling Kit (SP6/T7), Boehringer-Mannheim). After detection in alkaline phosphatase reaction buffer (Dig Nucleic Acid Detection Kit, Boehringer-Mannheim), the reaction was stopped by washing in 1× PBS. Antibody reactions were performed as recently described (Westerfield, 1994).

Detection of apoptotic cell death

Apoptotic cell death in zebrafish whole-mounts was detected according to a modification of the protocol suggested by the manufacturer (ApopTag *In situ* Apoptosis Detection Kit-Peroxidase; Oncor Inc.). Embryos were fixed in 4% paraformaldehyde in PBS, and stored in methanol at –20˚C. After rehydration in PBT (1× PBS, 0.1% Tween 20), embryos were permeabilized by a 15 minute digestion with proteinase K (10 μg/ml) in PBS and postfixed for 20 minutes in 4% paraformaldehyde in PBS. Subsequently, embryos were postfixed with prechilled (–20˚C) ethanol:acetic acid 2:1 and incubated for 1 hour at room temperature in equilibration buffer (provided in the ApopTag *In situ* Apoptosis Detection Kit-Peroxidase). After incubation over night at 37°C in working strength terminal deoxynucleotidyl transferase (TdT) enzyme, the DNA endlabelling reaction using digoxigenin-labelled dUTP was stopped by washing in stop/wash buffer. Digoxigenin-tagged DNA was detected using sheep anti-dioxigenin-alkaline phosphatase conjugated Fab fragments (Dig Nucleic Acid Detection Kit, Boehringer-Mannheim).

Photography and microscopy

For photographic documentation, live embryos were manually dechorionated with Dumont's no. 5 forceps and embedded in 1.5% methylcellulose in embryo medium (Westerfield, 1994).

Embryos stained after antibody reactions, whole-mount in situ hybridizations, or terminal deoxynucleotidyl transferase reactions were dehydrated in methanol, cleared for 30 minutes in benzylbenzoate: benzylalcohol (2:1) and mounted in Permount.

Specimens were examined using a Zeiss Axiophot microscope with Nomarski optics and Kodak Ektachrome 160T films. Individual pictures were assembled into composites using a scanner and Adobe Photoshop software.

JB-4 plastic metacrylate sections

Zebrafish whole-mounts stained by TdT reaction were dehydrated in ethanol and infiltrated over night at 4˚C in JB-4 infiltration resin (JB-4 embedding solution A containing 1g/100ml JB-4 catalyst; Polysciences Inc.). After embedding of specimen in JB-4 Infiltration Solution:JB-4 Hardener (25:1) and hardening of blocks over night at room temperature, specimens were sectioned transversally.

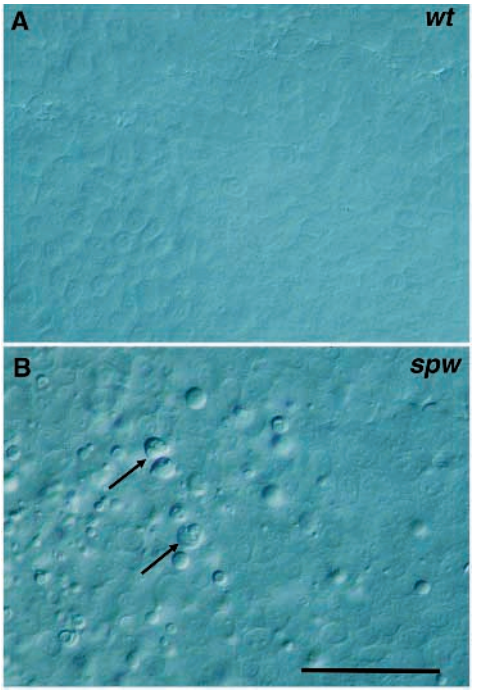

Fig. 4. Neuroepithelial tissues at 24 hpf. (A) Wild-type. (B) Morphology of dying cells in *space cowboy*^{m332}. Arrows indicate dying cells. Cells viewed with DIC optics. Scale bar, 25 μm.

RESULTS

A total of 481 mutations, almost one fifth of all mutations found during the screen, were identified by the presence of CNS-specific degeneration. Phenotypical analysis enables us to distinguish among three prominent categories. The first and largest category comprises 398 mutations that lead to massive and widespread CNS-specific cell death which becomes apparent only after somitogenesis and does not result in an abnormal brain morphology. Due to the abundance of these mutations, only a small subset of 16 mutations was maintained and will be presented together with 33 mutations of the second category at a later time. Mutations of the second category cause region-specific or transient CNS degeneration only after somitogenesis without displaying morphological abnormalities. Finally, a third category of 50 mutations that fall into the spacehead and fala-like classes cause early onset CNS degeneration during somitogenesis. Furthermore, mutant embryos of both classes have an abnormal brain morphology.

The spacehead class mutations result in early onset region-specific degeneration

Within the spacehead class of mutations, there are 43 independent isolates that define, at most, 30 complementation groups (Table 1). All of them are zygotic recessive mutations that lead to a characteristically altered brain morphology (Fig. 1B). At 28 hpf, most of the mutations lead to degeneration within the entire central nervous system (CNS), visible as regions of higher opacity.

The spacehead mutations are further divided into three phenotypic groups (Table 1). Group I comprises the most severely degenerating mutants, which are clearly smaller than wild-type embryos, have a slightly wavy posterior notochord, and have somites with slightly irregular borders at 28 hpf (Fig. 2D). At around the same time, mutant embryos show regions of degeneration outside of the neuroectoderm and usually degenerate completely within a few days. Group II and III mutations are characterized by degenerations of moderate and mild severity, respectively. While degenerations are very pronounced in neuroectodermal tissues, non-neural derivatives such as the notochord and somites appear not to be significantly affected as assessed by visual inspection of their morphology and the absence of opacity in these tissues (Figs 2C, 3E-H). Strikingly, several mutations of all three groups have a thinner yolk extension as an additional morphological feature (Fig. 3G). Although we have no explanation for this feature, we have noted that the time point at which the yolk extension begins to form (16 hpf) coincides with the spreading of cell death throughout the anteroposterior extent of the neuroectoderm. At 28 hpf, all of the mutants are touch responsive, indicating a functional circuitry of sensory neurons, interneurons, motoneurons and muscle cells. However, motor control appears to be affected, as less coordinated muscle contractions replace normal escape response movements.

Most of the mutations cause an enlargement of tectal and hindbrain ventricles by 28 hpf. Additionally, the telencephalon appears to be extended anteriorly, presumably due to an enlargement of the forebrain ventricle (Fig. 1B). Exceptional in this respect are group I mutations in which such an enlargement of brain ventricles is observed only at about 30-32 hpf.

Due to the phenotypic similarities within the three groups of spacehead mutations, five representative mutations (*uchu hikoushi*^{m172}, *saturn*^{m465}, *gumowy*^{m585}, *endeavor*^{m591} and *yura*^{m627}) were chosen for a more detailed analysis (for further analysis of cell-type- and region-specific markers see next sections). The earliest time point at which degeneration is apparent in mutations *uchu hikoushi*^{m172} and *saturn*^{m465} is the 6-7-somite stage (12 hpf). At the 10-somite stage (13 hpf), *gumowy*^{m585} and *yura*^{m627} display the first visible cell death. The early pattern of degeneration is comparable, in that all four mutations have foci of degeneration in hypothalamic and thalamic regions of the brain and in the eye (Fig. 3E,F). Regions of degeneration contain large numbers of rounded-up cell bodies (Fig. 4B), a morphology that is reminiscent of apoptotic cells in *C. elegans* (Sulston and Horvitz, 1977). Within the next 2 hours of development, degeneration spreads into the hindbrain and along the entire spinal cord. It is important to note that primarily regions within the neuroectoderm appear to be affected during somitogenesis. At the same time, mesodermal structures appear to develop normally as indicated by morphological differentiation markers of mesodermal structures, such as vacuolization of the notochord and chevron-shaping of somites (Fig. 3H). Furthermore, no increased numbers of degenerating cells are detectable within mesodermal tissues under the compound microscope with DIC optics.

Our observation that several spacehead mutations result in increased numbers of rounded-up cell bodies within degenerating regions, similar to apoptotic cells in *C. elegans*, led us to inquire whether the observed cell death might be apoptosis. Since the cellular morphology of dying cells is indicative of, but not sufficient as the sole criterion for apoptotic cell death, a detection assay for DNA fragmentation was employed to study a number of mutations. By using this assay, the 20-somite stage wild-type embryos display a dynamic pattern of cell death within the brain, spinal cord, non-neural tissues, and the tailbud (Fig. 5A). At later stages, around 28-30 hpf, wild-type embryos display a clearer pattern of naturally occurring cell death. Foci of increased cell death are present for example in the lens of the eye and the region of the trigeminal ganglion (data not shown). A small number of single dying cells is found in non-neural tissues.

At the 20-somite stage, all five spacehead mutations chosen for further analysis exhibit a pattern of dramatically increased DNA fragmentation within the brain and spinal cord (Fig. 5B). Histological sections of the trunk region demonstrate that dying cells are localized within the spinal cord (Fig. 5E). No bias has been detected with respect to localization of degenerating cells at a specific dorsoventral level within the spinal cord. Such a pattern of apoptotic cell death within the brain and spinal cord indicates a defect within the entire neuroectoderm. Levels of cell death within the non-neural tissues are comparable to wild-type embryos. In addition, some of the mutations such as *gumowy*^{m585} lead to slightly increased levels of cell death in the proliferative tailbud region (Fig. 5B).

At 28 hpf, spacehead mutant embryos maintain the same pattern of dramatically increased cell death that was present at the 20-somite stage, 10 hours earlier (data not shown). Some of the mutations lead to foci of increased cell death in the hindbrain and tectum. In addition to the neuroectodermal cell death, spacehead group I mutants have increased levels of dying cells in more ventral regions of the embryo. Cells dying in these regions might be neural crest, ectodermal, or mesodermal

Table 1. Complementation groups of mutations affecting neural survival

Genetic loci	Alleles	Phenotype	Other phenotypes	
spacehead class				
Group I				
zezem (zez)	*m97, m111, m307, m512*	Severe degeneration in CNS, large brain ventricles	No circulation	–
uchu hikoushi (uhi)	*m172, m476*	Same as above	No circulation, tail curved	–
interrail (itr)	*m221, m470, m680*	Same as above	Thin yolk extension	–
apollo (apo)	*m404, m491*	Same as above	Thin yolk extension	–
cudak (cud)	*m409, m432*	Same as above	Thin yolk extension	–
saturn (sat)	*m465*	Same as above	Weak circulation, thin yolk extension	–
neil (nel)	*m728*	Same as above	No circulation	–
voyager (voy)	*m766*	Same as above	–	–
Group II				
spazz (spz)	*m250*	Degeneration in CNS, large brain ventricles	Weak circulation, thin yolk extension	–
space cowboy (spw)	*m332, m541*	Same as above	Weak circulation	–
spaceman (spm)	*m333*	Same as above	Weak circulation	–
pan twardowski (ptw)	*m481*	Same as above	Thin yolk extension	–
galileo (gal)	*m492, m510*	Same as above	Weak circulation	–
major tom (maj)	*m506*	Same as above	–	–
enterprise (ent)	*m584*	Same as above	Thin yolk extension	–
gumowy (guw)	*m445, m585, m700*	Same as above	Weak circulation	–
eagle (egl)	*m691*	Same as above	–	–
hubble (hub)	*m727*	Same as above	–	–
–	*m488*	Same as above	Thin yolk extension	–
–	*m685*	Same as above	–	–
Group III				
viking (vik)	*m331*	Some degeneration in CNS, slightly enlarged brain ventricles	Thin yolk extension	–
solaris (sol)	*m461*	Same as above	Thin yolk extension	–
endeavor (end)	*m591*	Same as above	–	–
yura (yur)	*m479, m627*	Same as above	Weak circulation	–
kepler (kep)	*m733*	Same as above	Weak circulation	–
–	*m383*	Same as above	Thin yolk extension	–
–	*m513*	Same as above	–	–
–	*m514*	Same as above	Weak circulation, thin yolk extension	–
–	*m590*	Same as above	–	–
–	*m613*	Same as above	Thin yolk extension	–
fala-like class				
fala (faa)	*m83, m249*	Degeneration in CNS, brain ventricles reduced, hindbrain wavy	Body curved ventrally	–
deadhead (dhd)	*m175*	Degeneration in CNS, brain ventricles not inflated, wavy hindbrain	Weak circulation	–
flatbrain (flb)	*m224*	Degeneration in CNS, brain ventricles not inflated	No circulation	–
lost and found (lot)	*m236*	Degeneration in CNS, brain ventricles slightly reduced	–	–
beachboy (beb)	*m240*	Degeneration in CNS, brain ventricles not inflated, wavy hindbrain	Weak circulation	–
–	*m569*	Severe CNS degeneration, enlarged brain ventricles	–	–
Miscellaneous				
Group I				
skidmark (skm)	*m88*	Early degeneration of entire embryo	–	–
stop and drop (sad)	*m367, m486*	Early degeneration in anterior and trunk	–	–
frost (fst)	*m718*	Degeneration of entire embryo	–	–
goner (gon)	*m407*	Degeneration in CNS and tail	–	–
degenerant (dgn)	*m94, m372*	Degeneration in CNS and tail	–	–
Group II				
hörnle (hör)	*m274, m744*	Severe developmental delay between 11-15 somite stage	No circulation	–
stop it (sit)	*m745*	Same as above	–	–
pandora (pan)	*m313*	Same as above	Pleiotropic defects including heart, eyes, tail	a,b
Group III				
sideswipe (ssw)	*m762*	Early degeneration in the anterior	No circulation, tail and somite defects	–
anhalter (anh)	*m149, m403, m767*	Severe developmental delay followed by degeneration	–	–
orient express (ori)	*m769*	Degeneration in CNS and tail	–	–
gorp (gor)	*m776*	Same as above	–	–
cheerios (che)	*m285*	Developmental delay followed by degeneration	–	–
passing fancy (paf)	*m405*	Degeneration in CNS, large brain ventricles	Brain and tail defects	c
stop and die (snd)	*m254*	Anterior degeneration	–	–
quitter (qui)	*m206*	Same as above	–	–
Group IV				
pinatubo (pat)	*m560*	Possible periderm defect	–	–
bubbles (bub)	*m450*	Degeneration in anterior and tail	No circulation	–

Other phenotypic aspects of these mutations are described in: a, Malicki et al., 1996; b, Stainier et al., 1996; c, Stemple et al., 1996.

Mutations *gumowy*^{m445}, *hubble*^{m727}, and *beachboy*^{m240} were identified by generation of homozygous diploid embryos (Streisinger et al., 1981).

Complementation crosses were performed among all mutations within a class. Mutations of the miscellaneous class were tested only within the individual groups. Complementation among all loci with names has been completed. In the spacehead and fala-like classes, the crosses listed in the methods section were not tested.

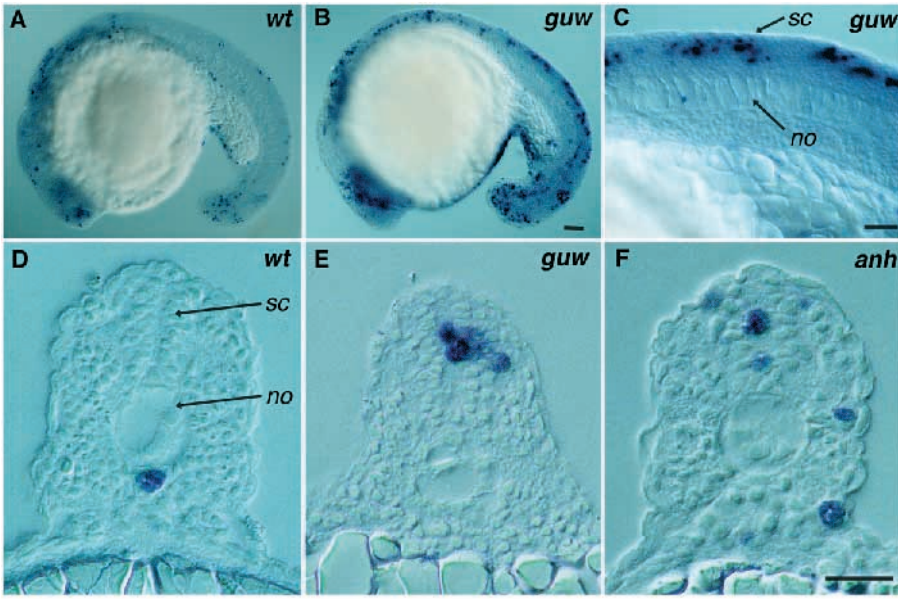

Fig. 5. DNA fragmentation in 20-somite stage embryos. (A,D) Wild-type. (B,C,E) *gumowy*^{m585}. DNA fragmentation is localized to the spinal cord and anterior neuroectoderm in mutant embryos. (F) *anhalter*^{m767}. DNA fragmentation is increased in all major embryonic tissues. (DF) Transverse sections at trunk level. Cells undergoing DNA fragmentation are stained blue. no, notochord; sc, spinal cord. Scale bars, (A,B) 100 μm, (C) 25 μm, (D-F) 25 μm.

derivatives. Nevertheless, the density of cell death within the neuroectoderm is markedly higher than in other tissues.

Phenotypic features of the fala-like class of mutations

The fala-like class of mutations contains seven mutations in, at most, six independent loci. Mutants in this phenotypically diverse class are characterized by visible degeneration within the brain and spinal cord by the late somite stages (Table 1). At 28 hpf, the mutants show either an abnormal hindbrain morphology or abnormal ventricle inflation ('fala' is Polish for wave which reflects the hindbrain morphology). Mutants *fala*^{m83} and *deadhead*^{m175} display strongly reduced brain ventricles (Fig. 1C). Moreover, the hindbrain region appears granular and in some instances bears a distinct wavy morphology. Mutant *flatbrain*^{m224} embryos have reduced brain ventricles, similar to *fala*^{m83}. Mutant *m569* embryos develop severe degeneration with inflated brain ventricles, and completely degenerate within 3 days. Finally, mutant *lost and found*^{m236} embryos have slightly enlarged brain ventricles. As seen in the spacehead class of mutations, all fala-like mutant embryos respond to tactile stimulation. Therefore, the neural circuitry involved in touch response appears to be present. All mutants within the fala-like class have severely increased levels of cell death within the neuroectoderm, similar to the spacehead mutants at 28 hpf.

Miscellaneous early degenerative mutations

To compare the tissue-specificity of degeneration found in the spacehead and fala-like classes, we analyzed a number of mutations leading to various types of apparently non-tissue-specific cell death. This class consists of 23 mutations in 18 independent loci (Table 1). Cell death in these mutant embryos is frequently accompanied by developmental retardation. Out of the more than 490 other degenerative or apparently non-tissue-specific mutations, the mutations were selected for their early onset of increased cell death. A common criterion of most mutant embryos is an onset of degeneration during somitogenesis, resulting in the disintegration of embryos within hours to a few days. In comparison, the differing pattern of nuclear fragmentation encountered in mutants of this class indicates that cell death in the spacehead and fala-like classes is CNS specific.

Mutants with an early degenerative phenotype (*skidmark*^{m88}, *stop and drop*^{m367}, *frost*^{m718}, *goner*^{m407}, and *stop and die*^{m254}) are exemplified by mutant *stop and drop*^{m367} which has degeneration within the anterior and in the trunk as early as the 3-somite stage (Figs 2F, 6B). At the 20-somite stage, dying cells are spread throughout all major embryonic tissues (Fig. 7C,D). Some mutants exhibit a developmental delay or degeneration commencing around or after the 15-somite stage (*sideswipe*^{m762}, *degenerant*^{m94}, *anhalter*^{m767}, *orient express*^{m769}, *gorp*^{m776}, *quitter*^{m206}, *cheerios*^{m285} and *passing fancy*^{m405}). At the 20-somite stage, *anhalter*^{m767} has increased cell death

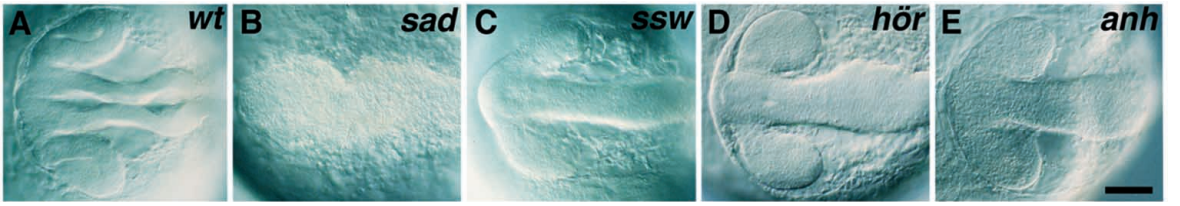

Fig. 6. Head phenotypes of miscellaneous early degeneration mutants. Dorsal view onto brain of 20-somite stage embryos. (A) Wild-type. (B) *stop and drop*^{m367}. (C) *sideswipe*^{m762}. (D) *hörnle*^{m274}. (E) *anhalter*^{m767}. Living embryos viewed with DIC optics, anterior to the left. Scale bar, 100 μm.

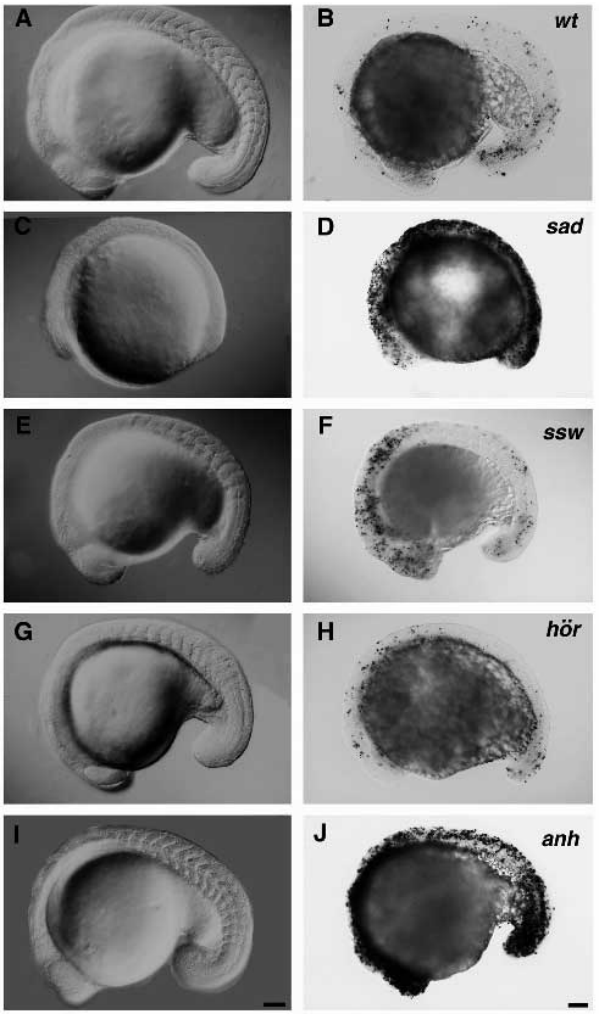

Fig. 7. DNA fragmentation in miscellaneous early degeneration mutants at the 20-somite stage. (A,B) Wild-type. (C,D) *stop and drop*^{m367}. (E,F) *sideswipe*^{m762}. (G,H) *hörnle*^{m274}. (I,J) *anhalter*^{m767}. (A,C,E,G,I) Lateral view of live embryos, viewed with DIC optics, anterior to the left. (B,D,F,H,J) Whole-mount staining for DNA fragmentation. Scale bars, 100 μm.

along the entire anteroposterior axis of the embryo within all major embryonic tissues (Figs 2G, 5F, 6E, 7I,J). Yet, *sideswipe*^{m762} mutant embryos display a more tissue-specific pattern of cell death (Figs 2E, 6C). In this mutant, DNA fragmentation in the anterior neuroectoderm sets in at the 14-somite stage, 2 hours prior to visible developmental delay. At the 20-somite stage, increased cell death is still restricted to the anterior neuroectoderm of the embryo (Fig. 7E,F).

A group of mutations in three loci abruptly delay embryonic development between the 11- to 15-somite stage (*hörnle*^{m274}, *pandora*^{m313}, and *stop it*^{m745}). *hörnle*^{m274} typifies this group, in that cell death sets in only after the 25-somite stage (Figs 2B, 6D). At the 20-somite stage, several hours after mutant embryos have become developmentally retarded, the assay for DNA fragmentation reveals no significantly increased cell death (Fig. 7G,H). Therefore, cell death appears not to be an immediate consequence of developmental retardation.

One mutant is notable with respect to its rapid disintegration around the 13-somite stage (*pinatubo*^{m560}). Apparently, disintegration of *pinatubo*^{m560} mutant embryos is caused by the disruption of the large yolk cell underlying the embryonic tissues. If kept in an isotonic solution, mutant embryos do not disintegrate rapidly, but instead show breaks within the periderm which progressively retracts over the yolk cell towards the embryo proper. This finding is consistent with the absence of significant levels of DNA fragmentation, revealing that this mutant is not apoptotic.

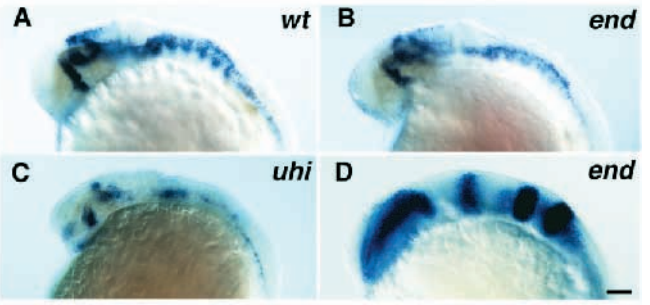

Fig. 8. Expression patterns of region-specific markers in spacehead mutant anterior neuroectoderm. (A-C) *hlx-1* expression at 28 hpf. (A) Wild-type. (B) *endeavor*^{m591}. (C) *uchu hikoushi*^{m172}. (D) Expression pattern of *pax a* and *b* and *krx-20* in *endeavor*^{m591} at the 10-somite stage is normal. Lateral view. Viewed with DIC optics, anterior to the left. Scale bar, 100 μm.

Hindbrain architecture in spacehead and fala-like mutants

We have analyzed five spacehead mutations using a variety of molecular markers to determine which cell types are affected by cell death. At the 10-somite stage, no abnormal patterning within the anterior CNS was observed as indicated by expression domains of *pax a* and *b*, and *krx-20* (Krauss et al., 1991; Oxtoby and Jowett, 1993) (Fig. 8D). In contrast, expression of *hlx-1* (Fjose et al., 1994) appears abnormal at 28 hpf (Fig. 8A-C). The *hlx-1* expression pattern at this stage is complex and comprises domains in almost all of the major subunits of the brain. The reduction of *hlx-1* expression in the spacehead mutants affects all regions equally, indicating that there is no region specific effect on *hlx-1* expression. Moreover, there is a clear correlation between phenotypic strength of the mutation and the degree to which *hlx-1* expression domains are reduced. Mutations resulting in the most marked cell degeneration have the strongest reduction of *hlx-1* expression. A similar reduction of *hlx-1* expression was found for several fala-like mutations (data not shown).

For further characterization of spacehead mutations, a number of antibodies were chosen that recognize specific subsets of neural cell types or label axon tracts. Islet-1 antibody labels cranial ganglia, Rohon Beard neurons, and ventromedial cells of the spinal cord (Thor et al., 1991; Korzh et al., 1993; Yamada et al., 1993). At 28 hpf, the number of trigeminal ganglion cells is reduced to half or even less than half of the normal cell number in two mutations from the spacehead group I (*uchu hikoushi*^{m172} and *saturn*^{m465}; Fig. 9C,D).

Radial glia in zebrafish are recognized by the zrf-1 antibody (Trevarrow et al., 1990). At 28 hpf, the staining pattern reveals a clear reduction of differentiated radial glia cells for all of the five spacehead mutations tested (Fig. 9E,F). Znp-1 antibody

recognizes primary motoneurons such as the CaP motoneuron (Eisen et al., 1986) in each somitic segment and a ladder array of longitudinal tracts with neuropils in each hindbrain segment (Trevarrow et al., 1990; Fig. 9A). All of the spacehead mutants tested have a single CaP motoneuron in each trunk and tail segment (data not shown). The hindbrain region, however, is clearly affected by the mutations in that, although the longitudinal fascicles are present, the neuropil of each hindbrain segment is reduced or nearly absent as assessed with the znp-1 antibody (Fig. 9B). Similarly, the staining pattern of the anti-acetylated tubulin antibody reveals an abnormal neuronal architecture within the hindbrain region in mutants of the spacehead and fala-like classes (Fig. 10B-F). The descending longitudinal tracts are present in mutant embryos, although they appear thinner and not as well fasciculated as in wild-type embryos. In wild-type embryos, the axons of commissural neurons were shown to cross the midline near the segment borders of each neuromere (Trevarrow et al., 1990). In contrast, in mutant embryos such as *saturn*^{m465}, individual axons appear to cross the midline in an irregular pattern. Furthermore, the compact bundles usually formed by these axons are less fasciculated and are reduced in size (Fig. 10D). Similar to the findings with the *hlx-1* expression domains, there is a clear correlation between phenotypic strength of the mutant and the degree to which the hindbrain axon tracts appear abnormal. One of the weakest spacehead mutants (*endeavor*^{m591}) shows an almost normal scaffold of hindbrain axon tracts (Fig. 10B). At this level of analysis, we have not been able to determine whether abnormal axon tracts are caused by specific defects of axon pathfinding or represent secondary effects of abundant cell death.

DISCUSSION

The spacehead and fala-like classes of mutations affect neural survival in zebrafish

Our large-scale mutagenesis screen for embryonic lethal mutations in zebrafish *Danio rerio* has led to the identification of a large number of mutations with significantly increased levels of cell death within the neuroectodermal lineages. Among the 481 mutations which cause cell death in the embryonic zebrafish CNS, 398 mutations result in an onset of widespread neural degeneration during the second day of development or later. These mutations appear to be similar to the *ned1*^{b39} mutation (Grunwald et al., 1988) and were not further studied. A second category of 33 mutations displays region-specific or transient neural degeneration phenotypes. They appear normal under visual inspection before the second day of development and will be described at a later time.

Here, we present mutations with early onset of increased cell death, well before the end of somitogenesis (24 hpf; Kimmel et al., 1995), and focus on mutations of the spacehead and fala-like classes. Mutations in these two classes were identified at 28 hpf on the basis of an altered brain morphology with either enlarged brain ventricles (spacehead class) and an abnormally shaped hindbrain, or abnormally inflated brain ventricles (fala-like class). Furthermore, high levels of cell death within the neuroectoderm are indicated by increased tissue opacity.

We investigated whether the increased cell death is apoptosis. Since neither nuclear DNA fragmentation nor cellular morphology, of dying cells are sufficient sole criteria for apoptotic cell death (Collins et al., 1992), we have applied both types of analysis. Our studies reveal that in the subset of five spacehead mutations analyzed, dying cells exhibit both a cellular morphology, reminiscent of *C. elegans* programmed cell death (Sulston and Horvitz, 1977), and DNA fragmentation, and might therefore die by an apoptotic mechanism. This finding is consistent with studies in *Drosophila melanogaster* showing that some developmental mutations lead to cell death by apoptosis (Abrams et al., 1993; White et al., 1994), and suggests that apoptosis might be the prominent mode of cell death during abnormal development. During the entire analysis, we have not been able to determine any separate mechanisms of cell death similar to the *C. elegans deg-1* mutation (Chalfie and Wolinsky, 1990).

The transparency of the zebrafish embryo has enabled us to observe dying cells in the living embryo by visual inspection. As of now, no other organism besides *C. elegans* has been shown to have this feature. Therefore, zebrafish is a potential model organism to study developmental cell death in the living vertebrate embryo. In this initial analysis, we have attempted to characterize neural cell death in mutant embryos. Observation of live animals and molecular analyses of degeneration in mutants of the spacehead and fala-like classes have revealed that dying cells are localized within the entire spinal cord, hindbrain, rostral brain, as well as the retina. Nevertheless, we have not been able to identify specific cell types affected by cell death. Our conclusion, that predominantly neural cell types are degenerating, is based on two lines of evidence: first, cell death is localized within neuroectodermal tissue of the embryo; and second, the dramatically increased level of cell death in spacehead mutants correlates with a reduced number of differentiated neuroectodermal cells that express either *hlx-1*, or present antigens recognized by the znp-1, zrf-1, or Islet-1 antibodies (the latter three recognizing predominantly primary motoneurons and radial glia). This indicates that a subset of these cells might have degenerated by the early pharyngula stages (24-28 hpf).

We have not been able to determine whether the reduced number of differentiated neuroectodermal cells is directly caused by degeneration or by proliferation or differentiation defects within the neuroectoderm. At 30 hpf, *hlx-1* expression in *uchu hikoushi*^{m172} is clearly reduced and displays similarities to the normal 22 hpf expression pattern (Fjose et al., 1994). Therefore, normal proliferation or differentiation of *hlx-1*-expressing cells might be delayed. Similarly, the reduced number of trigeminal neurons and radial glia might be caused by a developmental delay. Nevertheless, such a delay would be specific for the neuroectoderm since non-neural tissues appear to proliferate and differentiate properly.

To evaluate and compare the specificity of neural degeneration caused by spacehead and fala-like mutations, we present a number of mutants with widespread early cell death that were selected out of more than 490 early degenerative or apparently non-tissue-specific degenerative mutations. Comparison of histological sections of 20-somite stage *gumowy*^{m585} and *anhalter*^{m767} mutant embryos illustrates that the pattern of cell death in the spacehead mutant embryos is different from general widespread degeneration. We suggest that such a tissue-specific cell death is not caused by a general cell lethality. Furthermore, degeneration first becomes apparent in some spacehead mutations around the 7-somite stage (12 hpf) and spreads into regions outside of the CNS only by the end of somitogenesis (24-

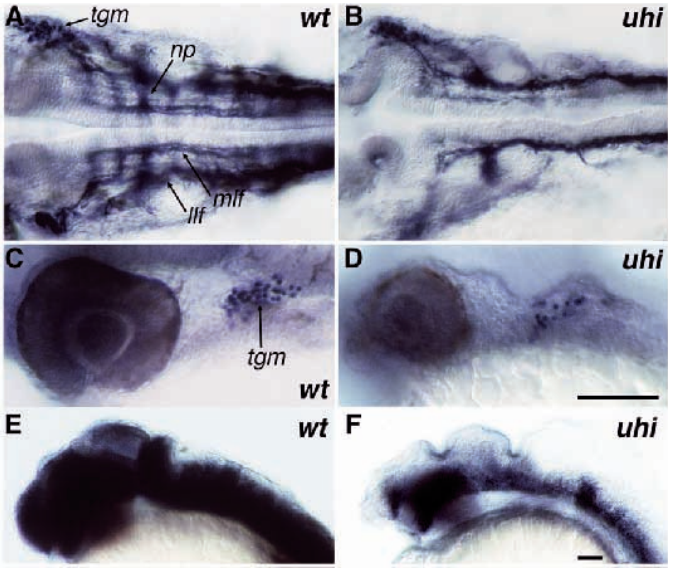

Fig. 9. Analysis of neural cell types in mutant *uchu hikoushi*^{m172} at 30 hpf. (A,C,E) Wild-type. (B,D,F) *uchu hikoushi*^{m172}. (A,B) Dorsal view of znp-1 antibody staining pattern in hindbrain region. Neuropils in each hindbrain segment are affected in mutants. (C,D) Lateral view of Islet-1 antibody staining pattern caudal to the eye. The number of trigeminal ganglion cells is reduced in mutant embryos. (E,F) Lateral view of zrf-1 antibody staining pattern in head region. Mutant embryos have severly reduced amounts of radial glia cells. np, neuropil in hindbrain segment; llf, lateral longitudinal fascicle; mlf, medial longitudinal fascicle; tgm, trigeminal ganglion. Scale bars, (A-D), 100 μm; (E,F) 100 μm.

28hpf). Such a long delay suggests that other tissues are affected only secondarily, perhaps as a result of extensive neuroectodermal degeneration. Alternatively, mutations might act on all cell types but the wild-type function of the genes might be less essential or required only at later stages outside of the CNS. This important question will have to be addressed in genetic mosaics by placing mutant non-neural cells into a wild-type background.

Possible genetic causes for the defects of the spacehead and fala-like classes of mutations

The spacehead class of mutations comprises a total of 43 mutations in, at most, 30 independent loci (Table 1). The distribution of alleles indicates that saturation for genes that can give rise to a similar phenotype has not been reached. With an average allele frequency of 1.4 alleles per locus, a good estimate of the number of genes in this class is not possible. However, it is conceivable that the entire class will consist of a limited number of genes. The large number of loci identified in this class of mutations would suggest that very similar phenotypes might be caused by a variety of distinct defects. Furthermore, it raises the question as to whether the spacehead mutations might be involved in the genetic control of related biological processes.

Due to the large number of spacehead mutations, it appears less likely that all mutations are defects in genes that control the suppression of cell death within the genetic cell death pathway such as *bcl-2* (Ellis and Horvitz, 1986; Hengartner and Horvitz, 1994). Furthermore, there is a lack of phenotypic similarities with *bcl*-2-deficient mice which are normal at birth. Only later, in mutant mice severe lymphoid apoptosis results in a breakdown of the immune system (Veis et al., 1993). Yet, some of the mutations might be defects within as yet unknown tissue-specific *bcl-2*-like genes or in genes that control the entry into the cell death pathway.

The phenotypic comparison of spacehead and fala-like mutant embryos with mouse mutants carrying targeted disruptions of members of the neurotrophin family signaling pathways reveals but few similarities. Neither the severe forms of massive cell death caused by the zebrafish mutations nor the morphological abnormalities, such as enlarged brain ventricles, have been described for the mouse mutants (Klein et al., 1993; Jones et al., 1994). Nevertheless, similar to some spacehead mutations (in particular *uchu hikoushi*^{m172} and *saturn*^{m465}), BDNF and *trk*B mutant mice have a reduced number of trigeminal neurons.

Mutations of the spacehead and fala-like classes might affect genes that are required for proper differentiation or maintenance of the various neural cell types, such as genes required for cell fate specification or encoding growth or differentiation factors. Thus, programmed cell death might appear as the default fate for cells that cannot complete their terminal differentiation. Furthermore, spacehead and fala-like mutations

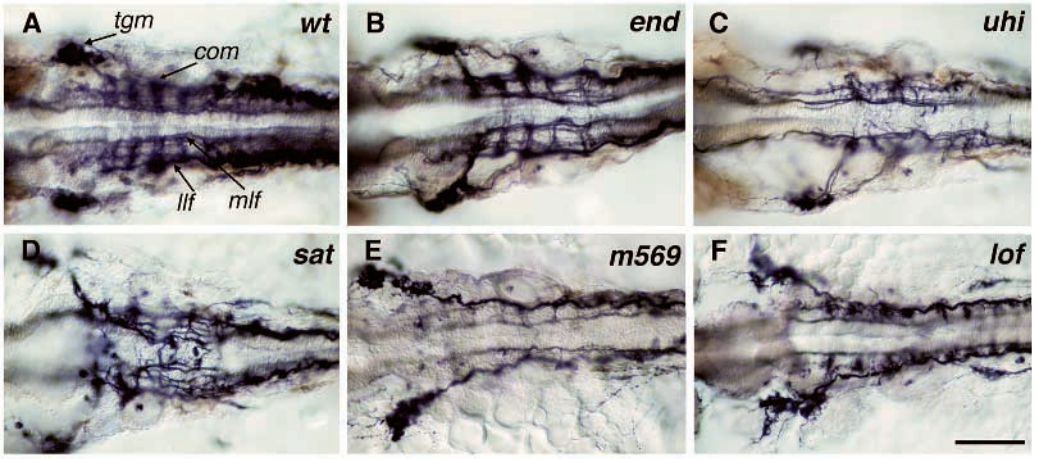

Fig. 10. Staining pattern of acetylated tubulin antibody in hindbrain region of spacehead and fala-like classes of mutants at 28 hpf. (A) Wild-type. Normal ladder array of longitudinal fascicles with commissural tracts in each hindbrain segment. (B) *endeavor*^{m591}. Mild phenotype. (C) *uchu hikoushi*^{m172}. (D) *saturn*^{m465}. (E) *m569.* (F) *lost and found*^{m236}. (B-F) Variability of mutant phenotypes. Longitudinal fascicles and commissural tracts are less fasciculated in mutants. Commissural tracts appear to be diminished or to cross the midline in aberrant positions. Dorsal view onto hindbrain. Viewed with DIC optics, anterior to the left. com, commissural tract; llf, lateral longitudinal fascicle; mlf, medial longitudinal fascicle; tgm, trigeminal ganglion. Scale bar, 100 μm.

might be defects in genes that are required for tissue-specific metabolic or physiological activities.

Considerations of possible secondary defects of the spacehead and fala-like classes of mutations

The intriguing finding that spacehead mutations give rise to ventricular phenotypes suggests that similar physiological processes that underlie the inflation of brain ventricles might be affected. In vertebrates, the normal inflation of brain ventricles is partially dependent on the choroid plexus, a secretory epithelium that produces cerebrospinal fluid (CSF; Davson et al., 1987). No structure related to the choroid plexus found in adult teleosts has been described in the embryonic zebrafish brain. However, the fact that normal inflation of brain ventricles has occurred by 28 hpf is indicative of the presence of a functionally similar structure.

In higher vertebrates, the fluid pressure within the brain ventricles is controlled by the secretion of the CSF from the choroid plexus and by the subsequent drainage of the CSF out of the ventricles traversing the subarachnoid spaces. In humans, defects such as degenerations, infections, or tumors that result in either oversecretion of CSF or obstruction of the drainage system lead to an increased fluid pressure. These defects have been implicated as major causes for hydrocephalus (Davson et al., 1987). Furthermore, in experimental animals hydrocephaly can be induced by injection of kaolin into the CSF. Kaolin causes an inflammation resulting in the obstruction of the cranial subarachnoid spaces (Del Bigio et al., 1994). Genetic evidence from newborn mice with polydactyly suggests that abnormal levels of apoptosis in brain regions such as the infralimbic cortical plate, hypothalamus and periventricular thalamus are causally linked with ventricular expansion and hydrocephaly (Keino et al., 1994).

The observation that all mutations in the spacehead class are characterized by early onset of degeneration within the CNS prior to morphological changes in the brain suggests that the ventricular expansion might be a secondary effect of early massive cell death. As a result, a common denominator within the spacehead class of mutations might be the impact on the same cell types or brain regions that are required for the maintenance of normal fluid pressure within the brain ventricles. Assuming that the fluid pressure in the embryonic zebrafish brain is at least partially regulated by the same mechanisms that control the fluid pressure in the adult brain, we suggest that the mutations resulting in enlarged brain ventricles might lead to defects analogous to those causing hydrocephaly in humans and other vertebrates.

Some experimental and genetic evidence indicates that the extent of blood flow through the choroid plexus influences the amount of secretion of CSF and thereby the enlargement of the neural tube and brain ventricles (Carey and Vela, 1974; Weiss and Wertman, 1978; see also Schier et al., 1996). In the spacehead class of mutations we have observed enlarged brain ventricles in a number of mutations with missing or reduced circulation, such as *saturn*^{m465} or *neil*^{m728}. This finding suggests that in spacehead mutant embryos the enlargement of brain ventricles is not dependent on a normal blood flow. In contrast, the failure to secrete CSF as a result of reduced circulation or enzymatic or structural defects within the secretory cells of a structure, functionally similar to the choroid plexus might account for the failure of brain ventricles in mutants of the fala-like or fullbrain classes to inflate (see also Schier et al., 1996).

Conclusion

The mutations described here might provide a genetic framework to aid in the understanding of the activation of inappropriate programmed cell death in a vertebrate system. Future analysis might open additional entry points into the etiology of degenerative and physiological disorders within the CNS.

We thank Colleen Boggs, Jane Belak, Lisa Vogelsang, Ioannis Batjakas, Jeanine Downing, Heather Goldsboro, Lisa Anderson, Xiaorong Ji, Snørri Gunnarson, and Kristen Diffenbach for technical help during the various stages of the screen. Thanks to Pamela Cohen, Michal Reichman, and Junying Yuan for critical reading of an earlier version of the manuscript. Kristen White gave helpful advice during the project. We would like to thank our collaborators A. Fjose, T. Jessel, T. Jowett, S. Krauss and B. Trevarrow for kindly providing in situ probes and antibodies. This work was supported in part by NIH RO1-HD29761 and a sponsored research agreement with Bristol Myers-Squibb (to W. D.). Further support in the form of fellowships came from HSFP and the Fullbright Program (to Z. R.), EMBO and Swiss National Fond (to A. S.), Helen Hay Whitney Foundation (to D. L. S. and D. Y. S.), the Medical Research Council of Canada (to M. H.), and the Damon Runyon-Walter Winchell Cancer Research Fund (to J. M.).

REFERENCES

Abrams, J. M., White, K., Fessler, L. I. and Steller, H. (1993). Programmed cell death during *Drosophila* embryogenesis. *Development* **117**, 29-43.

Barde, Y.-A. (1989). Trophic factors and neuronal survival. *Neuron* **2**, 1525-1534.

Carey, M. E. and Vela, A. R. (1974). Effect of systemic arterial hypotension on the rate of cerebrospinal fluid formation in dogs. *J. Neurosurg.* **41**, 350-355.

Chalfie, M. and Wolinsky, E. (1990). The identification and suppression of inherited neurodegeneration in *Caenorhabditis elegans*. *Nature* **345**, 410-416.

Chang, G.-Q., Hao, F. and Wong, F. (1993). Apoptosis: final common pathway of photoreceptor death in *rd*, *rds*, and rhodopsin mutant mice. *Neuron* **11**, 595-605.

Choi, D. W. (1992). Excitotoxic cell death. *J. Neurobiol.* **23**, 1261-1276.

Cohen, S. R., Levi-Montalcini, R. and Hamburger, V. (1954). A nerve growth-stimulating factor isolated from sarcomas 37 and 180. *Proc. Natl. Acad. Sci. USA* **40**, 1014-1018.

Collins, R. J., Harmon, B. V., Gobe, G. C. and Kerr, J. F. (1992). Internucleosomal DNA cleavage should not be the sole criterion for identifying apoptosis. *J. Rad. Biol.* **61**, 451-453.

Crowley, C., Spencer, S. D., Nishimura, M. C., Chen, K. S., Pitts-Meek, S., Armanini, M. P., Ling, L. H., McMahon, S. B., Shelton, D. L., Levinson, A. D. and Philipps, H. (1994). Mice lacking nerve growth factor display perinatal loss of sensory and sympathetic neurons yet develop basal forebrain cholinergic neurons. *Cell* **76**, 1001-1011.

Davson, H., Keasley, W. and Segal, M. B. (1987). *Physiology and Pathophysiology of the Cerebrospinal Fluid.* New York: Churchill Livingstone.

Del Bigio, M. R., da Silva, M. C., Drake, J. M. and Tuor, U. I. (1994). Acute and chronic cerebral white matter damage in neonatal hydrocephalus. *Can. J. Neurol. Sci.* **21**, 299-305.

Driever, W., Solnica-Krezel, L., Schier, A. F., Neuhauss, S. C. F., Malicki, J., Stemple, D. L., Stainier, D. Y. R., Zwartkruis, F., Abdelilah, S., Rangini, Z., Belak, J. and Boggs, C. (1996). A genetic screen for mutations affecting embryogenesis in zebrafish. *Development* **123**, 37-46.

Eisen, J. S., Myers, P. Z. and Westerfield, M. (1986). Pathway selection by growth cones of identified motoneurons in live zebrafish embryos. *Nature* **320**, 269-71.

Ellis, H. M. and Horvitz, H. R. (1986). Genetic control of programmed cell death in the nematode *C. elegans*. *Cell* **44**, 817-829.

Ellis, R. E., Yuan, J. and Horvitz, H. R. (1991). Mechanisms and functions of cell death. *Ann. Rev. Cell Biol.* **7**, 663-698.

Ernfors, P., Lee, K.-F. and Jaenisch, R. (1994). Mice lacking brain-derived neurotrophic factor develop with sensory deficits. *Nature* **368**, 147-150.

Fjose, A., Izpisua-Belmonte, J. C., Fromental-Ramain, C. and Duboule, D. (1994). Expression of the zebrafish gene *hlx-1* in the prechordal plate and during CNS development. *Development* **120**, 71-81.

Gavrieli, Y., Sherman, Y. and Ben-Sasson, S. A. (1992). Identification of programmed cell death in situ via specific labeling of nuclear DNA fragmentation. *J. Cell Biol.* **119**, 493-501.

Grunwald, D. J., Kimmel, C. B., Westerfield, M., Walker, C. and Streisinger, G. (1988). A neural degeneration mutation that spares primary neurons in the zebrafish. *Dev. Biol.* **126**, 115-28.

Hamburger, V. and Levi-Montalcini, R. (1949). Proliferation, differentiation and degeneration in the spinal ganglia of the chick embryo under normal and experimental conditions. *J. Exp. Zool.* **111**, 457-501.

Hamburger, V. (1992). History of the discovery of neuronal death in embryos. *J. Neurobiol.* **23**, 1116-1123.

Hengartner, M. O. and Horvitz, H. R. (1994). The *C. elegans* cell survival gene *ced-9* encodes a functional homolog of the mammalian proto-oncogene *bcl-2*. *Cell* **76**, 665-676.

Jessel, T. M. (1991). Neuronal survival and synapse formation. In *Principles of Neural Science* (ed. Kandel, E. R., Schwartz, J. H. and Jessel, T. M.), pp. 929-944. New York: Elsevier.

Jones, K. R., Farinas, I., Backus, C. and Reichardt, L. F. (1994). Targeted disruption of the BDNF gene perturbs brain and sensory neuron development but not motor neuron development. *Cell* **76**, 989-999.

Keino, H., Masaki, S., Kawarada, Y. and Naruse, I. (1994). Apoptotic degeneration in the arhinencephalic brain of the mouse mutant *Pdn/Pdn*. *Brain Res. Dev. Brain Res.* **78**, 161-168.

Kerr, J. F. R., Wyllie, A. H. and Currie, A. R. (1972). Apoptosis: a basic biological phenomenon with wide ranging implications in tissue kinetics. *Br. J. Cancer* **26**, 239-257.

Kimmel, C. and Westerfield, M. (1990). Primary neurons of the zebrafish. In *Signals and Sense* (ed. Edelman, G., Gall, W. and Gowan, W.), pp. 561-588. New York: Wiley Liss.

Kimmel, C. B., Ballard, W. W., Kimmel, S. R., Ullmann, B. and Schilling, T. F. (1995). Stages of embryonic development of the zebrafish. *Dev. Dyn.* **203**, 253-310.

Klein, R. (1994). Role of neurotrophins in mouse neuronal development. *FASEB J.* **8**, 738-744.

Klein, R., Smeyne, R. J., Wurst, W., Long, L. K., Auerbach, B. A., Joyner, A. L. and Barbacid, M. (1993). Targeted disruption of the *trk*B neurotrophin receptor gene results in nervous system lesions and neonatal death. *Cell* **75**, 113-122.

Klein, R., Silos-Santiago, I., Smeyne, R. J., Lira, S. A., Brambilla, R., Bryant, S., Zhang, L., Snider, W. D. and Barbacid, M. (1994). Disruption of the neurotrophin-3 receptor gene *trk* C eliminates Ia muscle afferents and results in abnormal movement. *Nature* **368**, 249-251.

Korzh, V., Edlund, T. and Thor, S. (1993). Zebrafish primary neurons initiate expression of the LIM homeodomain protein Isl-1 at the end of gastrulation. *Development* **118**, 417-425.

Krauss, S., Johansen, T., Korzh, V. and Fjose, A. (1991). Expression pattern of zebrafish pax genes suggests a role in early brain regionalization. *Nature* **353**, 267-270.

Lee, K.-F., Li, E., Huber, L. J., Landis, S. C., Sharpe, A. H., Chao, M. V. and Jaenisch, R. (1992). Targeted mutation of the gene encoding the low affinity NGF receptor p75 leads to deficits in the peripheral sensory nervous system. *Cell* **69**, 737-749.

Levi-Montalcini, R. W. (1987). The nerve growth factor: thirty-five years later. *EMBO J.* **6**, 1145-1154.

Malicki, J., Neuhauss, S. C. F., Schier, A. F., Solnica-Krezel, L., Stemple, D. L., Stainier, D. Y. R., Abdelilah, S., Zwartkruis, F., Rangini, Z. and Driever, W. (1996). Mutations affecting development of the zebrafish retina. *Development* **123**, 263-273.

Mullins, M. C., Hammerschmidt, M., Haffter, P. and Nüsslein-Volhard, C. (1994). Large-scale mutagenesis in the zebrafish: in search of genes controlling development in a vertebrate. *Curr. Biol.* **4**, 189-202.

Norman, D. J., Feng, L., Cheng, S. S., Gubbay, J., Chan, E. and Heintz, N. (1995). The *lurcher* gene induces apoptotic death in cerebellar Purkinje cells. *Development* **121**, 1183-1193.

Oppenheim, R. W. (1991). Cell death during development of the nervous system. *Ann. Rev. Neurosci.* **14**, 453-501.

Oxtoby, E. and Jowett, T. (1993). Cloning of the zebrafish *krox-20* gene (*krx-20*) and its expression during hindbrain development. *Nucl. Acids Res.* **21**, 1087-1095.

Raff, M. C. (1992). Social controls on cell survival and cell death. *Nature* **356**, 397-400.

Raff, M. C., Barres, B. A., Burne, J. F., Coles, H. S., Ishizaki, Y. and Jacobson, M. D. (1993). Programmed cell death and the control of cell survival: Lessons from the nervous system. *Science* **262**, 695-700.

Robertson, A. and Thomson, N. (1982). Ultrastructural study of cell death in *Caenorhabditis elegans*. *J. Embryol. Exp. Morphol.* **67**, 89-100.

Saunders, J. W. (1966). Death in embryonic systems. *Science* **154**, 604-612.

Schier, A. F., Neuhauss, S. C. F., Harvey, M., Malicki, J., Solnica-Krezel, L., Stainier, D. Y. R., Zwartkruis, F., Abdelilah, S., Stemple, D. L., Rangini, Z., Yang, H. and Driever, W. (1996). Mutations affecting the development of the embryonic zebrafish brain. *Development* **123**, 165-178.

Schwartz, L. M. and Osborne, B. A. (1994). *Ced-3*/ICE: Evolutionarily conserved regulation of cell death. *BioEssays* **16**, 387-389.

Smeyne, R. J., Klein, R., Schnapp, A., Long, L. K., Bryant, S., Lewin, A., Lira, S. A. and Barbacid, M. (1994). Severe sensory and sympathetic neuropathies in mice carrying a disrupted Trk/NGF receptor gene. *Nature* **368**, 246-249.

Solnica-Krezel, L., Schier, A. F. and Driever, W. (1994). Efficient recovery of ENU-induced mutations from the zebrafish germline. *Genetics* **136**, 1401-20.

Stainier, D. Y. R., Fouquet, B., Chen, J.-N., Warren, K. S., Weinstein, B. M., Meiler, S., Mohideen, M.-A. P. K., Neuhauss, S. C. F., Solnica-Krezel, L., Schier, A. F., Zwartkruis, F., Stemple, D. L., Malicki, J., Driever, W. and Fishman, M. C. (1996). Mutations affecting the formation and function of the cardiovascular system in the zebrafish embryo. *Development* **123**, 285-292.

Steller, H. (1995). Mechanisms and genes of cellular suicide. *Science* **267**, 1445-1449.

Stemple, D. L., Solnica-Krezel, L., Zwartkruis, F., Neuhauss, S. C. F., Schier, A. F., Malicki, J., Stainier, D. Y. R., Abdelilah, S., Rangini, Z., Mountcastle-Shah, E. and Driever, W. (1996). Mutations affecting development of the notochord in zebrafish. *Development* **123**, 117-128.

Streisinger, G., Walker, C., Dower, N., Knauber, D. and Singer, F. (1981). Production of clones of homozygous diploid zebrafish (*Brachydanio rerio*). *Nature* **291**, 293-296.

Sulston, J. E. and Horvitz, H. R. (1977). Post-embryonic cell lineages of the nematode, *Caenorhabditis elegans*. *Dev. Biol.* **56**, 110-156.

Thoenen, H. (1991). The changing scene of neurotrophic factors. *Trends Neurosci.* **14**, 165-170.

Thompson, C. B. (1995). Apoptosis in the pathogenesis and treatment of disease. *Science* **267**, 1456-1462.

Thor, S., Ericson, J., Brännström, T. and Edlund, T. (1991). The homeodomain LIM protein Isl-1 is expressed in subsets of neurons and endocrine cells in the adult rat. *Neuron* **7**, 881-889.

Trevarrow, B., Marks, D. L. and Kimmel, C. B. (1990). Organization of hindbrain segments in the zebrafish embryo. *Neuron* **4**, 669-679.

Truman, J. W. (1984). Cell death in invertebrate nervous systems. *Annu. Rev. Neurosci* **7**, 171-188.

Vaux, D. L., Haecker, G. and Strasser, A. (1994). An evolutionary perspective on apoptosis. *Cell* **76**, 777-779.

Veis, D. J., Sorenson, C. M., Shutter, J. R. and Korsmeyer, S. J. (1993). *Bcl-2*-deficient mice demonstrate fulminant lymphoid apoptosis, polycystic kidneys and hypopigmented hair. *Cell* **75**, 229-240.

Weiss, M. H. and Wertman, N. (1978). Modulation of CSF production by alterations in cerebral perfusion pressure. *Arch. Neurol.* **355**, 27-29.

Westerfield, M. (1994).*The Zebrafish Book*. Oregon, USA: University of Oregon Press.

White, K., Grether, M. E., Abrams, J. M., Young, L., Farrel, K. and Steller, H. (1994). Genetic control of programmed cell death in *Drosophila*. *Science* **264**, 677-683.

Wyllie, A. H., Kerr, J. F. R. and Currie, A. R. (1980). Cell death: the significance of apoptosis. *Int. Rev. Cytol.* **68**, 251-306.

Wyllie, A. H. (1995). The genetic regulation of apoptosis. *Curr. Gen. Dev.* **5**, 97-104.

Yamada, T., Pfaff, S. L., Edlund, T. and Jessell, T. M. (1993). Control of cell pattern in the neural tube: motor neuron induction by diffusible factors from notochord and floor plate. *Cell* **73**, 673-686.

Yuan, J., Shaham, S., Ledoux, S., Ellis, H. M. and Horvitz, H. R. (1993). The *C. elegans* cell death gene *ced-3* encodes a protein similar to mammalian interleukin-1β-converting enzyme. *Cell* **75**, 641-652.

Zakeri, Z. F., Quaglino, D., Latham, T. and Lockshin, R. A. (1993). Delayed internucleosomal DNA fragmentation in programmed cell death. *FASEB J.* **7**, 470-478.

(Accepted 8 January 1996)